

its paramagnetic resonance spectrum consists of a very broad peak, 450 G wide, which is difficult to observe unless high concentrations are present. We were unable to directly observe this resonance.

After the crystals were photoconverted to the F^+ state with ultraviolet light, iron was observed in the 1^+ valence state. A large F^+ center resonance signal together with the Mn^{2+} and V^{2+} spectra were also observed. In order to detect the Fe^{1+} resonance, which consists of a single line occurring at $g=4.15$, measurements at temperatures of $20^\circ K$ or lower were necessary due to the short spin relaxation time.¹³ Using a heat treatment schedule similar to that used to obtain the states for the various curves in Fig. 1, both the F^+ center and Fe^{1+} resonance signals were observed to decrease in essentially the same manner as the decrease of the $500^\circ K$ thermoluminescence peak. After the crystals were heated above $650^\circ K$, no further luminescence was observed, and neither the F^+ center nor Fe^{1+} ESR spectra could be detected, indi-

cating that the crystals had returned to their original F state. The crystals could be cycled between these states repeatedly. This fact was also observed in the previously reported optical absorption measurements.¹⁰

Owing to the correlation obtained between the ESR and thermoluminescence measurements, it is our conclusion that Fe^{2+} ions constitute the traps responsible for the $500^\circ K$ glow peak. The conversion process



is driven to the right by light in the F band and to the left by the thermal release of electrons from the Fe^{1+} ions. A similar attempt to correlate changes in ESR signals with the glow curve peaks occurring below room temperature was unsuccessful. Except for a slight decrease in the F^+ line, no change in the ESR spectrum was observed following heat treatments between 77 and $298^\circ K$.

†Work supported by the U. S. Office of Naval Research and the National Science Foundation.

*Present address: Department of Physics, Oklahoma State University, Stillwater, Okla. 74074.

¹J. E. Wertz, P. Auzins, R. A. Weeks, and R. H. Silsbee, Phys. Rev. **107**, 1535 (1957).

²J. E. Wertz, G. S. Saville, L. Hall, and P. Auzins, Proc. Brit. Ceram. Soc. **1**, 59 (1964).

³B. Henderson and R. D. King, Phil. Mag. **13**, 1149 (1966).

⁴J. C. Kemp, J. C. Cheng, E. H. Izen, and F. A. Modine, Phys. Rev. **179**, 818 (1969).

⁵E. B. Hensley and R. L. Kroes, Bull. Am. Phys. Soc. **13**, 420 (1968).

⁶E. B. Hensley, W. C. Ward, B. P. Johnson, and R. L. Kroes, Phys. Rev. **175**, 1227 (1968).

⁷W. C. Ward and E. B. Hensley, Phys. Rev. **175**, 1230 (1968).

⁸B. P. Johnson and E. B. Hensley, Phys. Rev. **180**, 931 (1969).

⁹Y. Chen, W. A. Sibley, F. D. Srygley, R. A. Weeks, E. B. Hensley, and R. L. Kroes, J. Phys. Chem. Solids **29**, 863 (1968).

¹⁰L. A. Kappers, R. L. Kroes, and E. B. Hensley, Phys. Rev. B **1**, 4151 (1970).

¹¹G. F. J. Garlick and A. F. Gibson, Proc. Phys. Soc. (London) **A60**, 574 (1948).

¹²J. E. Wertz, J. W. Orton, and P. Auzins, J. Appl. Phys. **33**, 322 (1962).

¹³J. W. Orton, P. Auzins, J. H. E. Griffiths, and J. E. Wertz, Proc. Phys. Soc. (London) **78**, 554 (1961).

Energy Bands in Boron Nitride and Graphite

J. Zupan

J. Stefan Institute, University of Ljubljana, Ljubljana, Yugoslavia

(Received 13 September 1971)

The tight-binding approximation has been applied for calculation of the band structure of planar hexagonal crystal layers of graphite and boron nitride. The theoretical width of the valence band of 15.9 eV in graphite and the distance between the centers of π and σ band of 5.3 eV as obtained in the present calculation are in good agreement with Chalkin's experimental work yielding 15 and 5 eV, respectively. For boron nitride, the width of the energy gap and the width of the valence band were calculated to be 4.9 and 6.8 eV, respectively.

INTRODUCTION

Several authors¹⁻⁵ studied the electron structure of hexagonal boron nitride as early as 1950.

The studies are mainly made in comparison with graphite. According to these authors the width of the gap between the valence and conduction band in boron nitride is determined predominately by

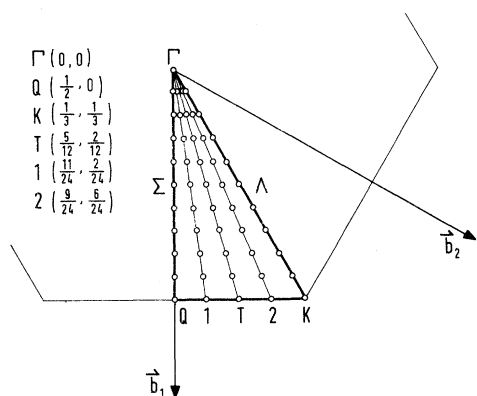


FIG. 1. Unit cell of the reciprocal space and the points in which the present calculation has been carried out.

π and not by σ electrons, although it is necessary to include both types of electrons in the calculation in order to get more precise information about the widths of bands and the shapes of density-of-states curves. In the present work energy bands of π and σ electrons for graphite and boron nitride are analyzed in a tight-binding⁶ approximation.

The structures of graphite and boron nitride contain only one type of strong bond, i. e., C-C and B-N bonds, respectively, joining each atom to its three coplanar nearest neighbors. The distances C-C and B-N in the same plane are 1.42 and 1.45 Å, respectively, whereas the distance between two atoms on neighboring planes is more than twice as large and the bonds are much weaker.^{2,5,7} In the present calculation, therefore, graphite and boron nitride are treated as a planar hexagonal one-layer crystal, except that in the treatment of π bonds the interactions between the neighboring planes were considered.

DESCRIPTION OF CALCULATION

The energy-band calculations were carried out using the program developed by Grad and Breb-

TABLE I. Different directions and points at which the present two-dimensional calculations were made together with their corresponding weight factors (\vec{b}_1 and \vec{b}_2 are unit vectors in k space).

Direction	Weight	No. of points
Point Γ	1	1
$s\vec{b}_1$ $0 \leq s \leq \frac{1}{2}$	6	10
$s(\vec{b}_1 + \vec{b}_2)$ $0 \leq s \leq \frac{1}{3}$	6	10
$s(5\vec{b}_1 + 2\vec{b}_2)$ $0 \leq s \leq \frac{1}{12}$	12	10
$s(11\vec{b}_1 + 2\vec{b}_2)$ $0 \leq s \leq \frac{1}{24}$	12	10
$s(9\vec{b}_1 + 6\vec{b}_2)$ $0 \leq s \leq \frac{1}{24}$	12	10

ner,⁸ which has been slightly modified for the present purpose. This program enables one to solve the secular equations with the complex matrix elements which appear in the energy calculations for the points with lower symmetries. The calculations were carried out for 51 points lying in different directions in \vec{k} space (Fig. 1). By symmetry these points give a mesh of 481 points in the first Brillouin zone. All these directions are listed in Table I. The basic potentials of atomic orbitals were obtained by the self-consistent-field (SCF) CNDO/2 method,⁹ taking into account the influence of the nearest three neighbors. The complete-neglect-of-differential-overlap (CNDO) method and the basic approximations of this method are discussed precisely in the same reference.⁹ According to Pople, Santry, and Segal,¹⁰ and Pople and Segal¹¹ the elements of the matrix representation of the Hartree-Fock Hamiltonian operator F in the secular equation

$$\sum_{\mu} (F_{\mu\nu} - \epsilon_i \delta_{\mu\nu}) C_{i\mu} = 0$$

were approximated with the expressions of Eqs. (1) and (2):

$$F_{\mu\mu} = -\frac{1}{2}(I_{\mu} + A_{\mu}) + [(P_{AA} - Z_A) - \frac{1}{2}(P_{\mu\mu} - 1)]\gamma_{AA} + \sum_{B \neq A} (P_{BB} - Z_B)\gamma_{AB}, \quad (1)$$

$$F_{\mu\nu} = -\beta_{AB}^0 S_{\mu\nu} - \frac{1}{2}P_{\mu\nu}\gamma_{AB}, \quad (2)$$

where $P_{\mu\nu}$ is an element of the density matrix P and γ_{AB} is a two-center integral approximated by the Matega^{12,13} approximation. The overlap integrals $S_{\mu\nu}$ were taken from the tables.¹⁴

The potentials of different atomic orbitals obtained by the CNDO/2 method which were used in this calculation are listed in Table II. All the calculations were made on a CDC 3300 electronic computer.

RESULTS AND DISCUSSION

The real problem in the tight-binding calculations is the introduction of the atomic-orbital po-

TABLE II. Potentials used in present calculations. VOIP's and electronegativities were used also to obtain SCF CNDO/1 and CNDO/2 potentials, respectively (energies in eV).

Atomic orbital	CNDO/2 potentials	VOIP	Electronegativity $-\frac{1}{2}(I_{\mu} + A_{\mu})$
2s(B)	-9.10	-14.05	-9.594
2s(C)	-14.99	-19.44	-14.051
2s(N)	-21.51	-25.58	-19.316
2p(B)	-4.87	-8.30	-4.001
2p(C)	-7.16	-10.67	-5.572
2p(N)	-9.77	-13.19	-7.275

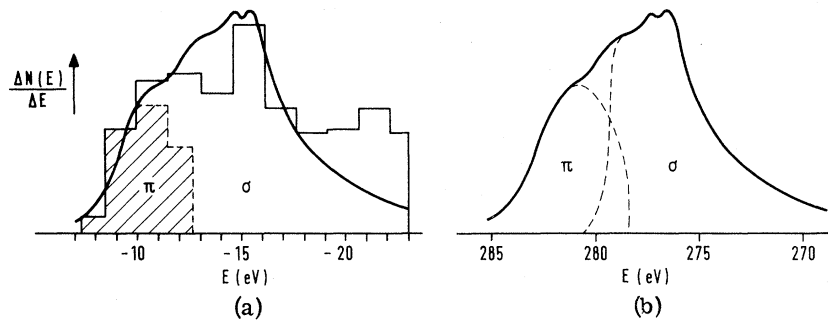


FIG. 2. (a) Density-of-states histogram prepared from data at 481 points in the first Brillouin zone with a sample size of $\Delta E = 1.5$ eV comparing with the Chalkin's experimentally obtained K -emission band in graphite. (b) Separation of the experimental curve on π and σ regions proposed by Coulson and Taylor.

tentials and exchange potentials. In the case of boron nitride for which no precise experimental data of band or forbidden-gap width are known [except Larach and Shrader's luminescence measurements¹⁵ and recently Vilanove's¹⁶ measurements on dielectric constant $\epsilon_2(\omega)$], it is very difficult to choose the "right" potentials to compare them with the calculated values. It was decided to make the same calculations for graphite having a very similar structure as boron nitride, with four different kind of potentials: with valence-state ionization potentials (VOIP) and with electronegativities taken from literature^{17,18} as well as with potentials calculated with SCF methods CNDO/1 and CNDO/2.^{10,11,18} From Chalkin's¹⁹ experimental data and Coulson and Taylor's theoretical considerations² of the graphite valence band, we obtained two starting points to compare them with our calculation. First, the width of the π region and the width of the whole valence band (π and σ regions) should be about 5.5 and 15 eV, respectively. Secondly, the centers of the occupied π and σ regions should differ by about 5 eV. The best agreement with the experimental data is obtained in the case of CNDO/2 potentials. The resulting density-of-states histogram together with Chalkin's experimental density-of-states curve and Coulson and Taylor's separation on π and σ regions are shown in Figs. 2(a) and (b), respec-

tively. The total width of the valence band obtained is 15.9 eV and the width of the π region is 5.3 eV. The difference between the centers of occupied π and σ regions is 5.3 eV, which is in good agreement with the starting points obtained from the experimental results.

In the calculated density-of-states histogram shown in Fig. 2(a) there is also a third peak which could not be detected in the experimental curve. The origin of this peak is due to the 2s electrons. The functions for lower-energy levels of the filled band have the character of the atomic s functions around the nucleus. However, the coefficients of the wave functions of p -type atomic orbitals are on the average about three times smaller than the coefficients of s -type atomic orbitals. Thus the transition probability for K -emission spectra became considerably smaller for lower-energy values than for higher ones.^{20,18} The comparison of Chalkin's experimental data (K emission of graphite) and some theoretically obtained values of different authors are given in Table III. The recent experimental work on graphite by Balzarotti and Grandolfo²¹ and Greenaway *et al.*²² show the occurrence of two peaks located at about 5 and 6 eV. Experimental and theoretical values obtained by different authors are shown in Table IV. Painter and Ellis,²³ and Bassani and Parravicini²⁴

TABLE III. Comparison between the experimental and calculated data for graphite (all values in eV).

	Total valence-band width	Width of π region	Difference between centers of π and σ regions
Experimental	15	5.5	5
Bassani and Parravicini (Ref. 24)	14.0	5.0	
Yamazaki (Ref. 20)	16	1	4.6
Painter and Ellis (Ref. 23)	19.3	7.3	
Lomer (Ref. 26)	12.5	5.0	
Present calc.	15.9	5.3	5.3

TABLE IV. Experimentally and theoretically obtained optical transitions in graphite.

	Reference	Position of peak (eV)	
Expt.	Balzarotti and Grandolfo (Ref. 21)	5.11	5.95
	Greenaway <i>et al.</i> (Ref. 22)	4.8	6.2
Theoret.	Painter and Ellis (Ref. 23)	4.6	
	Bassani and Parravicini (Ref. 24)	4.5	6.0
	Present calc.	5.1	6.0

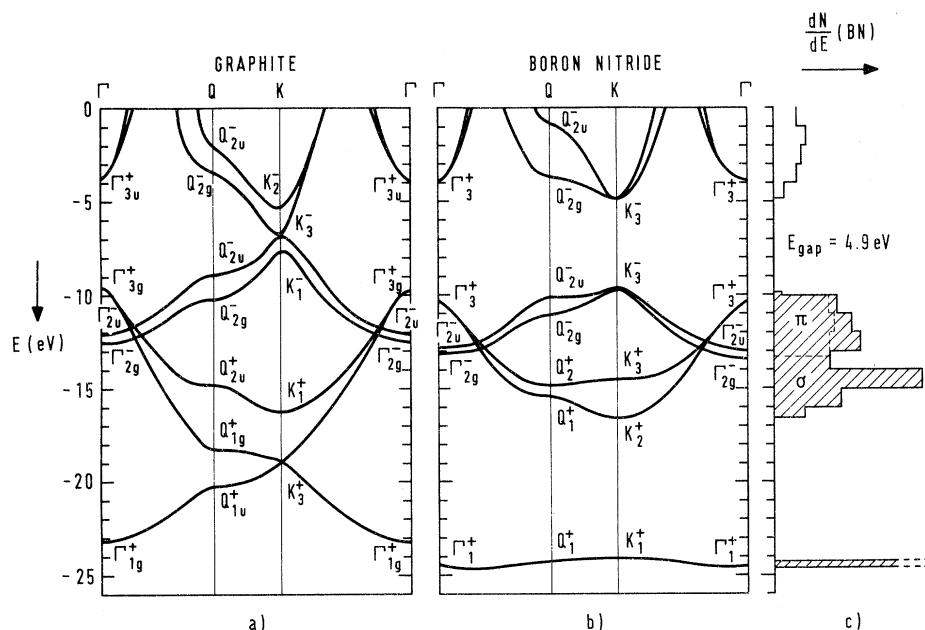


FIG. 3. Energy bands along the principal symmetry directions for hexagonal crystals of graphite and boron nitride. (The σ bands were calculated for two-dimensional crystals and the interaction between the neighboring layers in the π bands calculation was considered.)

conclude from theoretical considerations that the transition between the π bands at the point Q corresponds to the first maximum in the thermorefectance measurements located at 5 eV. Painter and Ellis considered the second peak at about 6 eV to be the result of the structure in the π bands near Q , while Greenaway *et al.* ascribe it to the zone-center ($\Gamma_{3g}^+ - \Gamma_{3u}^+$) transition. In the present calculation the energy difference between the points Γ_{3g}^+ and Γ_{3u}^+ is 6.0 eV, which is very near the value determined experimentally. There is also a theoretical consideration of van Haeringen and Junginger²⁵ who predicted a number of transitions, but there is no experimental evidence to date.

Since fairly satisfactory agreement was obtained with graphite, the same SCF CNDO/2 calculation was performed for boron and nitrogen atoms surrounded by three nitrogen or three boron atoms, respectively, in order to obtain the potentials for energy-band calculations. These potentials are listed in Table II and results of energy-band calculation for boron nitride are shown in Fig. 3(b) and 3(c).

As pointed out by several authors^{2,5,26} the only qualitative difference between boron nitride and graphite energy-band structures occurs in the point K . The degeneracy at this point in the case of graphite is due to the fact that both different sites in the unit cell, A and B , are occupied with the same kind of atoms. In the case of boron nitride the sites are occupied with the different atoms and hence the symmetry operation $\{I|f\}$ which produces the degeneracy is absent. The energy gap

in this point for boron nitride was determined in the present calculation to be 4.9 eV [Fig. 3(c)].

As expected the inclusion of the interaction between the nearest-neighbor planes via p_z electrons removes the degeneracy in the valence and conduction bands along some directions in k space. The results of the three-dimensional calculation for boron nitride are shown in Fig. 4. The calculation was made in a similar way as explained by Doni and Parravicini.⁵ The difference between their and our treatment of the problem is in the choice of the potentials used in the final calculation. The reducing factors were used in Doni and Parravicini's work, in order to obtain satisfactory

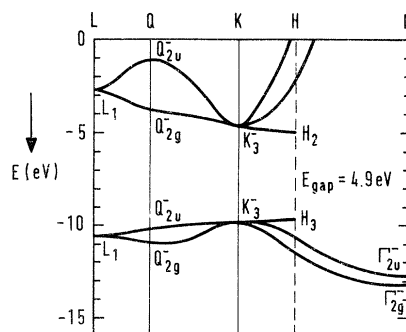


FIG. 4. Energy bands for three-dimensional π -electron structure in boron nitride. The potentials and overlap integrals used for this calculation are the same as for two-dimensional case. The coordinates of the points L and H in the \vec{k} space are as follows: $L(\frac{1}{2}, 0, \frac{1}{2})$ and $H(\frac{1}{3}, \frac{1}{3}, \frac{1}{2})$.

potentials and overlap integrals. On the other hand, we calculated the potentials of boron and nitrogen atoms on their positions in the lattice with the self-consistent-field CNDO method and these potentials were used in the band calculations. The positions of boron, nitrogen, and carbon atoms in one-layer hexagonal lattices of boron nitride and graphite are very similar to those of the organic systems such as borazole and anthracene. From this point of view, we have chosen the CNDO method, which is relatively simple and gives quite good potentials and electronic densities in organic closed-shell systems.⁹ It is therefore clear that the differences between Doni and Parravicini's and our calculation are only quantitative rather than qualitative.

In the three-dimensional case the energy gap in boron nitride is no longer at the point *K* (5.3 eV), but at the point *H* and has a value of 4.9 eV which can be compared with Larach and Shrader's¹⁵ minimal value of 5.5 eV obtained from the luminescence measurements. The width of the π region in the valence band amounts to 3.6 eV and the total width of the valence band is 6.8 eV. The measurements which were made recently by Vilanove¹⁶ on the dielectric constant of boron nitride show the position of the first peak of ϵ_2^j at 6.5 eV and the gap somewhere below 5 eV. It can be seen from Fig. 4 that the energy difference of 6.4 eV between the points Q_{2g}^+ and Q_{2u}^- agrees fairly well with the value experimentally obtained. In his work Vilanove also pointed out that he could not detect the duplication of this peak as reported

in the literature.²⁷ The first peak of ϵ_2^j at 9.4 eV which is compatible with the $\pi \rightarrow \sigma$ or $\sigma \rightarrow \pi$ transitions can be compared with the energy difference obtained by present calculations between the points Q_{2g}^+ and Q_{2g}^- [Fig. 3(b)] having a value of 11 eV.

Generally, the tight-binding method gives quite good agreement for the occupied (valence) bands, but it is of little use for highest (conduction) bands as explained by several authors.^{26,28-30} Due to the very large overlap integrals of excited orbitals, their atomic character in the Bloch sum is almost completely lost. The energy values are very sensitive to the overlap estimation; i. e., a small change in overlap integrals would produce a large change in energy values for the conduction bands.

In the present work it was shown that some experimental results can be interpreted on the basis of the tight-binding model using the potentials obtained by the SCF method. However, for making more thorough comparison with optical-transition data, the tight-binding approximation based on Slater-type wave functions seems to be rather crude.

ACKNOWLEDGMENTS

The author wishes to thank Dr. D. Kolar, Dr. S. Svetina, and Dr. P. Gosar for encouragement during the work and for many useful discussions. The author is also grateful to J. Grad and C. Trampuž for their help in computation of the results.

¹K. Ariyama and S. Mase, *Busseiron Kenkyu* **33**, 109 (1950).

²C. A. Coulson and R. Taylor, *Proc. Phys. Soc. (London)* **A65**, 815 (1952); **A65**, 834 (1952).

³K. Ariyama and S. Mase, *Progr. Theoret. Phys. (Kyoto)* **12**, 244 (1954); **12**, 246 (1954).

⁴V. Halpren, *J. Phys. Chem. Solids* **24**, 1495 (1963).

⁵E. Doni and G. P. Parravicini, *Nuovo Cimento* **B64**, 117 (1969).

⁶F. Bloch, *Z. Physik* **52**, 555 (1928).

⁷R. S. Pease, *Acta Cryst.* **5**, 356 (1952).

⁸J. Grad and M. A. Brebner, *Commun. Assoc. Computing Machinery* **11**, 820 (1968).

⁹J. A. Pople and D. L. Beveridge, *Approximate Molecular Orbital Theory* (McGraw-Hill, New York, 1970), p. 75.

¹⁰J. A. Pople, D. P. Santry, and G. A. Segal, *J. Chem. Phys.* **43**, S129 (1965).

¹¹J. A. Pople and G. A. Segal, *J. Chem. Phys.* **43**, S137 (1965).

¹²J. M. Sichel and M. A. Whithead, *Theoret. Chim. Acta* **11**, 220 (1968).

¹³N. Mataga, *Bull. Chem. Soc. Japan* **31**, 453 (1958).

¹⁴R. S. Mulliken, C. A. Rieke, D. Orloff, and H. Orloff, *J. Chem. Phys.* **17**, 1248 (1949).

¹⁵S. Larach and R. E. Shrader, *Phys. Rev.* **104**, 68 (1956).

¹⁶R. Vilanove, *Compt. Rend.* **B272**, 1066 (1971). The author is grateful to Dr. E. Doni, who brought his attention to this work.

¹⁷H. Basch, A. Viste, and H. B. Gray, *Theoret. Chim. Acta* **3**, 358 (1965).

¹⁸A. Morita, *Sci. Rept. Res. Inst. Tohoku Univ. Ser. A* **33**, 92 (1949).

¹⁹F. C. Chalkin, *Proc. Roy. Soc. (London)* **A194**, 42 (1948).

²⁰M. Yamazaki, *J. Chem. Phys.* **26**, 930 (1957).

²¹A. Balzarotti and M. Grandolfo, *Phys. Rev. Letters* **20**, 9 (1968).

²²D. L. Greenaway, G. Harbeke, F. Bassani, and E. Tosatti, *Phys. Rev.* **178**, 1340 (1969).

²³G. S. Painter and D. E. Ellis, *Phys. Rev. B* **1**, 4747 (1970).

²⁴F. Bassani and G. P. Parravicini, *Nuovo Cimento* **B50**, 95 (1967).

²⁵W. van Haeringen and H. G. Junginger, *Solid State Commun.* **7**, 1723 (1969).

²⁶W. M. Lomer, *Proc. Roy. Soc. (London)* **A227**, 330 (1955).

²⁷E. Doni and G. R. Parravicini, *Nuovo Cimento* **B64**,

117 (1969); Ref. 11.

²⁸R. H. Parmenter, *Phys. Rev.* **86**, 552 (1952).²⁹J. C. Slater, *Handbuch der Physik*, edited by S.

Flügge (Springer, Berlin, 1956), p. 27.

³⁰J. M. Ziman, *Principles of the Theory of Solids* (Cambridge U. P., Cambridge, England, 1965), p. 84.

PHYSICAL REVIEW B

VOLUME 6, NUMBER 6

15 SEPTEMBER 1972

Optics of Polaritons in Bounded Media

Joseph L. Birman*

*Laboratoire de Physique des Solides, Faculté des Sciences
and Groupe de Physique des Solides, Ecole Normale Supérieure,
Université de Paris, Paris V, France*

and

John J. Sein†

Physics Department, New York University, University Heights, Bronx, New York 10453

(Received 13 July 1970; revised manuscript received 13 December 1971)

Using a simple polarization picture of a medium in which there is spatial dispersion and using the integral equation method of Ewald-Oseen, some rigorous results are obtained for the optics of a bounded spatially dispersive medium. In particular, an extinction theorem for polaritons, and rigorous additional boundary conditions are obtained. The normal-incidence propagation of transverse modes for an isotropic crystal bounded by a plane is analyzed. The rigorous boundary conditions obtained by this method, in general, do not agree with other popular choices, based upon the same constitutive relations.

I. INTRODUCTION

The purpose of this paper is to give a simple derivation of results needed for an analysis of wave propagation in a bounded medium in which there is a nonlocal constitutive equation. Physically the nonlocality can arise from an exciton absorption lying close to the frequency of the propagating wave. This produces a wave-vector-dependent dielectric function and leads to propagation of the mixed exciton-photon modes known as polaritons.¹⁻³

When an incident plane wave impinges upon such a medium from vacuum, several polaritons can be excited in the medium. In a particular geometry these propagate parallel to the incident wave, but with different phase velocities. The total field consists of incident plus reflected fields in vacuum, plus the polariton fields in the medium. To determine the amplitudes of all fields, we need a complete set of boundary conditions. In addition the polariton dispersion relation for waves propagating in the medium is required. Finally, in order that the incident wave shall not propagate in the medium, we require an extinction condition.

The method we use to solve this problem is based on the Ewald-Oseen integral equation formulation of optics, plus a polarization picture of the spatially dispersive medium.⁴ In this framework the results can be derived in a particularly transparent fashion, and a comparison with the

treatments of the usual "local" optics can be made.

The extinction theorem, and the boundary conditions were first obtained by one of us⁵ using a somewhat different method. That derivation along with detailed numerical analysis and comparison of calculated and experimental reflectivity will be published separately. The calculated reflectivity is in satisfactory agreement with experiment.

The results of our analysis have been used in recent theoretical work on Raman scattering⁶ in the polariton picture. There, a quantum-mechanical treatment of polariton scattering inside the crystal, plus the polariton reflectivity at the crystal boundary was needed in order to compute cross sections for Raman scattering.

Besides being relatively simple and familiar, the method we use to analyze wave propagation is rigorous. It does not require, for example, that the surface boundary conditions be assumed, but yields them as a result of the theory. We return to this point later.

II. SPATIAL DISPERSION

Some field vectors needed in our work are $\vec{E}(\vec{r}, t)$ the macroscopic electric field and $\vec{P}(\vec{r}, t)$ the dielectric polarization at (\vec{r}, t) . The time and space Fourier transforms are defined as

$$\vec{P}(\vec{r}, \omega) = (1/(2\pi)^{1/2}) \int \vec{P}(\vec{r}, t) e^{-i\omega t} dt \quad (2.1)$$

$$\text{and} \quad \vec{P}(\vec{k}, \omega) = (1/(2\pi)^{3/2}) \int \vec{P}(\vec{r}, \omega) e^{-i\vec{k}\cdot\vec{r}} d\vec{r}. \quad (2.2)$$